Heliyon 5 (2019) e02909

Contents lists available at ScienceDirect

Heliyon

journal homepage: www.cell.com/heliyon

Research article

Effect of the molar concentration of pyrrole monomer on the rate of polymerization, growth and hence the electrochemical behavior of highly pristine PPy flexible electrodes

A.V. Thakur, B.J. Lokhande *

School of Physical Sciences, PAH Solapur University, Solapur, 413 255, M.S., India

ARTICLE INFO

Keywords:
Electrochemistry
Materials science
Materials chemistry
Physics
PPy
Electrochemistry
Molar concentration
Polymerization
Flexible electrodes
Materials synthesis
Surface chemistry

ABSTRACT

The rate of polymerization decides growth and hence electrochemical properties of the electrodes of conducting polymers synthesized by SILAR method are affected by molar concentration of the precursors. Present work describes the effect of molar concentration of Pyrrole monomer on the rate of polymerization and hence the electrochemical performance of highly pristine PPy flexible electrodes. 304 grade flexible stainless steel strips were coated with the PPy using aqueous solutions of 0.025M, 0.05 M and 0.1M pyrrole in 0.5 M H_2SO_4 separately and 30% H_2O_2. XRD patterns substantiate the formation of amorphous PPy. The peak at 1560 cm^{-1} in FTIR confirms the formation of polypyrrole. SEM images of the FEs prepared using different molar concentration shows gradual superficial growth. All FEs were electrochemically analyzed for their supercapacitive performance by the electrochemical techniques like cyclic voltammetry, galvanostatic charge discharge study and electrochemical impedance spectroscopy. It was found that, the specific capacitance increases with molar concentration of pyrrole. The pristine PPy FEs prepared with 0.1 M Pyrrole exhibit specific capacitance as high as 899.14 Fg^{-1} at 5 mVs^{-1} in 0.2 M Na_2SO_4.

1. Introduction

Electrically conducting polymers (ECPs) are attracting the researchers working on the materials for charge storage devices [1]. ECPs like polypyrrole (PPy) [2, 3], polyaniline (PANI) [4], polyethylene dioxy thiophene (PEDOT), polythiophene (PTh) and poly (3-Methylthiophene) (PMET)) [5] etc. have been being used as electrode materials for supercapacitors in pure [6, 7, 8, 9] as well as composite forms [10]. PPy is easy to synthesize, is conductive due to conjugated electrons, it can store charge throughout the bulk and is stable against thermal variations. The monomer pyrrole is water soluble. Thus PPy is more preferable among all of the ECPs for charge storage applications. Recently we have prepared highly pristine PPy flexible electrodes using pyrrole (Py) and H_2O_2 by SILAR technique [6]. Physical and chemical properties of SILAR grown thin films are greatly affected by different synthesis parameters such as molar concentration of precursors [11], dip time, dip cycles [12, 13], volume of precursors, synthesis bath temperature [14] etc. In continuation to our previous work, we have decided to study the impact of the molar concentration of the Py consumed during the SILAR synthesis on the rate of polymerization and hence the electrochemical performance of the highly pristine PPy FEs various analytical techniques and electrochemical techniques.

2. Experimental

2.1. Materials

For the present work, extra pure pyrrole (Py) (Sigma Aldrich) while 30% H_2O_2, H_2SO_4, HNO_3 and Na_2SO_4 (SD Fine chemicals) and these are used without further purification. Stainless steel Strips (SS) of 304 grades (1 $cm \times$ 5cm) were used as the conducting substrate material. 0.5 M H_2SO_4 was used as dispersion medium during the synthesis. All the solutions used were prepared using double distilled water as solvent.

2.2. Methods

Synthesis involves following steps.

2.2.1. Substrate cleaning and pretreatment

The flexible SS strips were mirror polished to get the rough surface using the emery polish paper (600 grade). This is followed by ultrasonication in double distilled water for 30 min These SS strips were

* Corresponding author.
E-mail address: bjlokhande@yahoo.com (B.J. Lokhande).

https://doi.org/10.1016/j.heliyon.2019.e02909
Received 10 May 2019; Received in revised form 4 July 2019; Accepted 20 November 2019

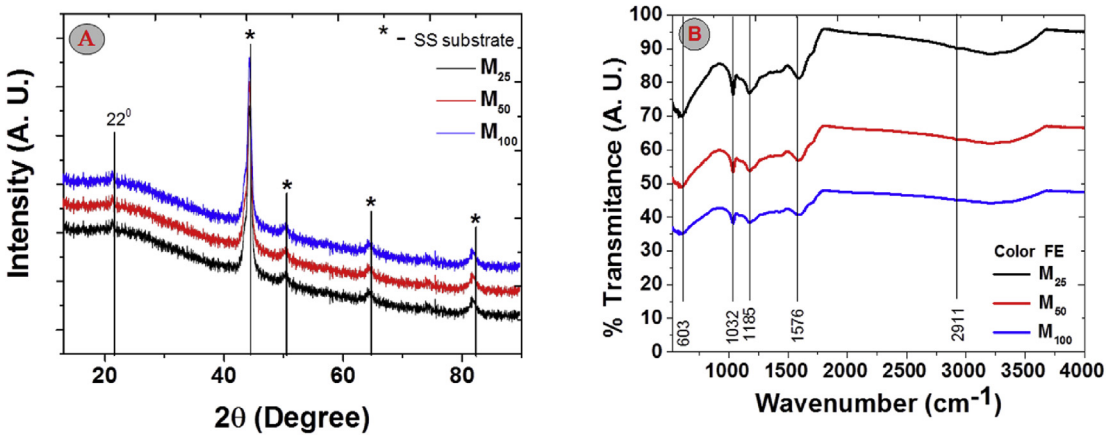

Fig. 1. A. XRD patterns of FEs M_{25}, M_{50} and M_{100}. B. FTIR spectra of FEs M_{25}, M_{50} and M_{100}.

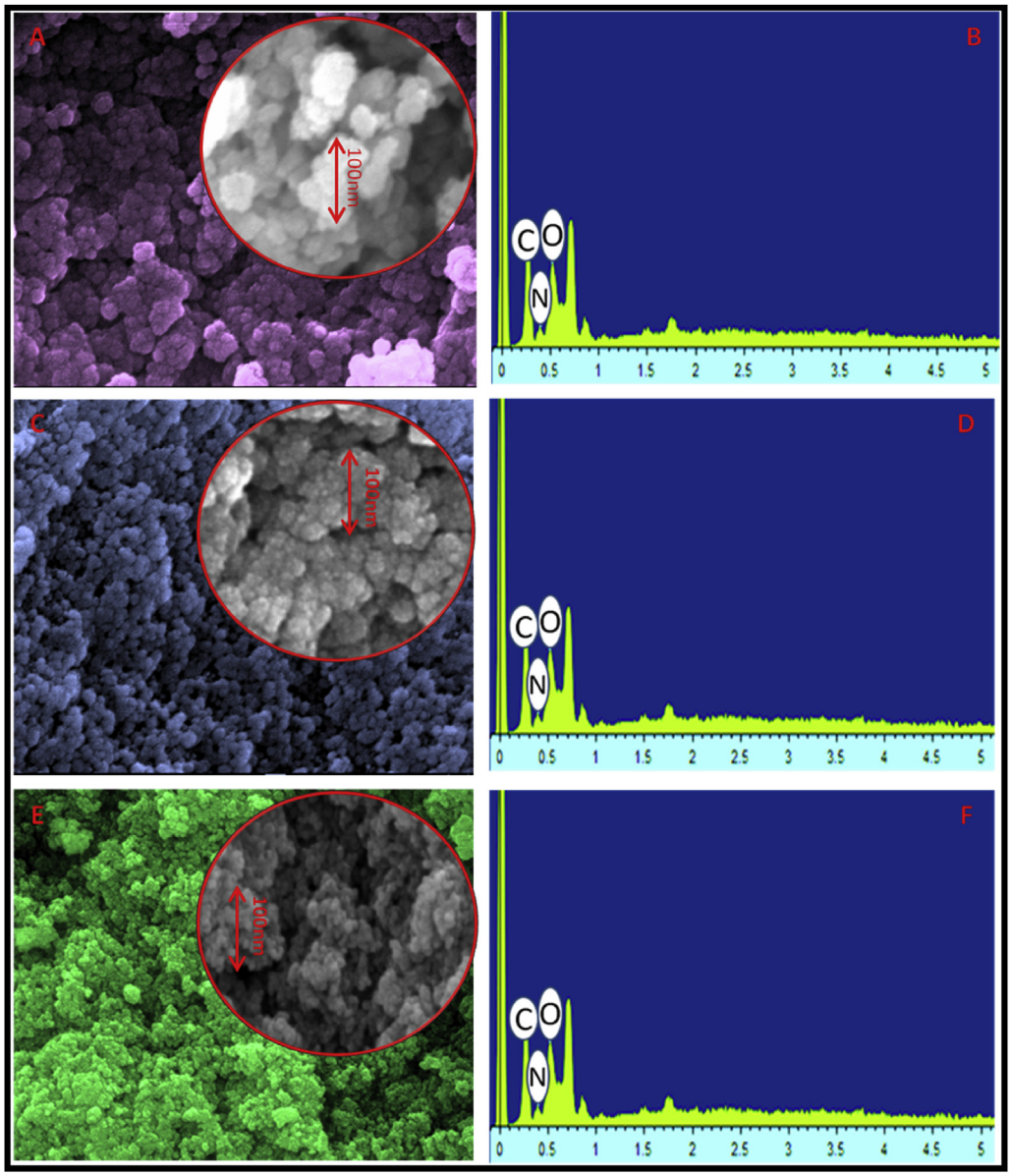

Fig. 2. A,C and E SEM images of FEs M_{25}, M_{50} and M_{100}. B,D and F EDX patterns of FEs M_{25}, M_{50} and M_{100}.

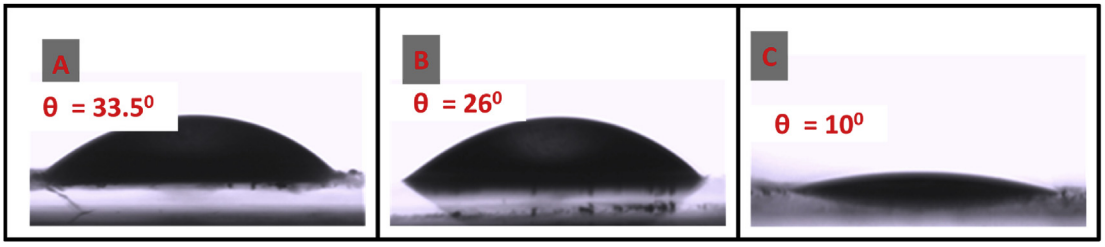

Fig. 3. A,B and C surface wettability analyses of FEs M_{25}, M_{50} and M_{100}.

immersed in 50 ml solution of 5 mM HNO_3 as the Pyrrole cations are adherent to the stainless steel treated with 5 mM HNO_3 for 15 min [6].

2.2.2. Preparation of the flexible electrodes

In the SILAR synthesis, SS strips were first immersed in 0.1M pyrrole (Py), and then in 30% H_2O_2 for 10s each. This is followed by pressure cleaning with jets of double distilled water. This completes one SILAR deposition cycle. 10 such SILAR cycles have been carried out to form uniform flexible electrodes (FEs). The flexible electrodes prepared with 0.025 M, 0.05 M and 0.1 M concentrations of Py monomer were labeled as M_{25}, M_{50}, and M_{100} respectively.

2.3. Characterizations

The XRD study of FEs M_{25}, M_{50}, and M_{100} was carried out by using X-ray diffractometer (Ultima IV Rigaku D/max2550Vb+18 kw with CuKα, λ = 1.54056 Å). FTIR study of the FEs M_{25}, M_{50}, and M_{100} was carried out by using the FTIR spectrophotometer (Nicolet iS10, Thermo Scientific, USA). Mass of the active material was measured by analytical microbalance (Tapson 100 TS) with least count 10^{-5} g. Scanning electron microscopic (SEM) analyses were carried out by using cold gun field emission scanning electron microscope (SEM JEOL JSM- 7600F HITACHI, Japan) to check the surface morphologies of different FEs.

Electrochemical analyzer (CHI 408C, CH Instruments USA) with standard three electrodes cell was used for electrochemical characterizations in which along with working electrode, platinum wire was used as a counter electrode whereas the saturated Ag/AgCl was used as a reference electrode and 0.2 Na_2SO_4 was used as electrolyte. Using $1cm^2$ area of the prepared electrode as electro-active material, electrochemical parameters were calculated using cyclic voltammetery (CV) chronopotentiometry (CP) and electrochemical impedance spectroscopy (EIS) of nearly 1 cm^2 surface area of the deposit.

3. Results and discussion

3.1. Film formation mechanism

Polymerization of Py to PPy is a well known process and has been described in literature [6]. In the acidic precursor solution pyrrole forms polaron by losing conjugated electron. The polarons are successively attached together to form bi-polaron, trimer, quenoid structure and finally the polymer called PPy.

3.2. Structural elucidation

The XRD patterns of the optimized FEs M_{25}, M_{50}, and M_{100} are shown in Fig. 1A. No peaks other than substrate material are observed. This explains the formation of amorphous PPy. As the formed material is amorphous, variations in the peak intensities are not seen.

FEs M25, M50 and M100 demonstrates the peak at wavenumber 1576 cm^{-1} corresponding to the characteristic C–C and C=C ring vibrations while the peak at 1032 cm^{-1} is due to C–H deformation vibration. The peak at 1185 cm^{-1} corresponds to C–N stretching, while the peak at 603 cm^{-1} is due to N–H wagging. The broad peak at 2911 cm^{-1} may be due to N–H stretching and vibrations (Fig. 1B). These peaks in FTIR spectra confirm the formation of highly pristine PPy. With increase in molar concentration of Py monomer, the rate of polymerization is increased. This increased the amount of material grown on the SS substrate and hence increases the thickness of FEs. The increased thickness results in increased absorbance and hence the fall of transmittance from M25 to M100 was observed. Figure 2A, C and E shows the SEM images of FEs M25, M50 and M100 successively. M25 exhibits globular morphology. The globules become smaller (from ~25nm to ~20nm) with increase in the molar concentration of pyrrole monomer. Figure 2B, D and F shows the EDX analyses of the FEs M25, M50 and M100 successively. The peaks corresponding to C and N are confirming the formation of PPy. The surface wettability measurements of FEs M_{25}, M_{50}, and M_{100} have been

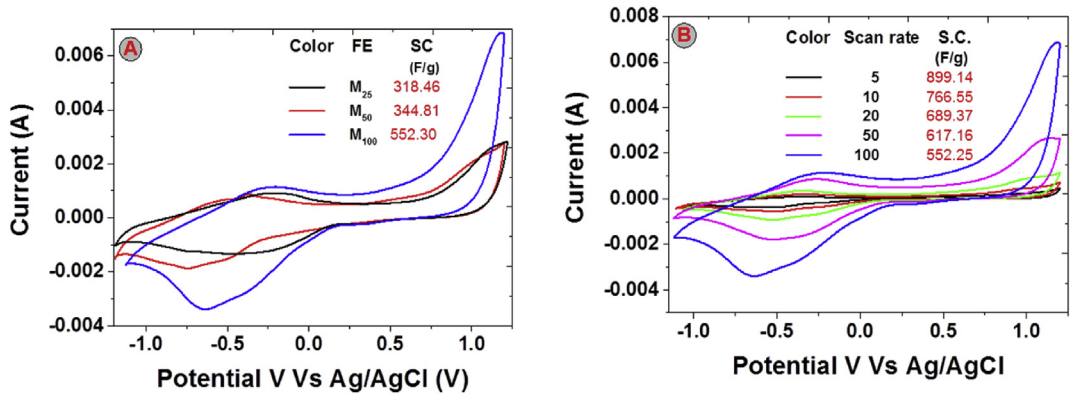

Fig. 4. A. Cyclic voltammograms of FEs M_{25}, M_{50} and M_{100} at 100 mV/s. B. Cyclic voltammograms of M_{100} at different scan rates.

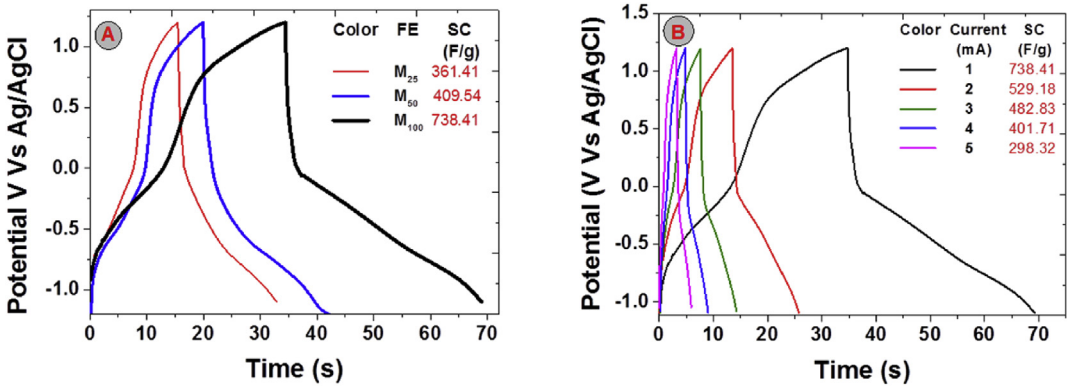

Fig. 5. A. GCD curves of FEs FEs M_{25}, M_{50} and M_{100} at 1mA. B. GCD curves of M_{100} at different currents.

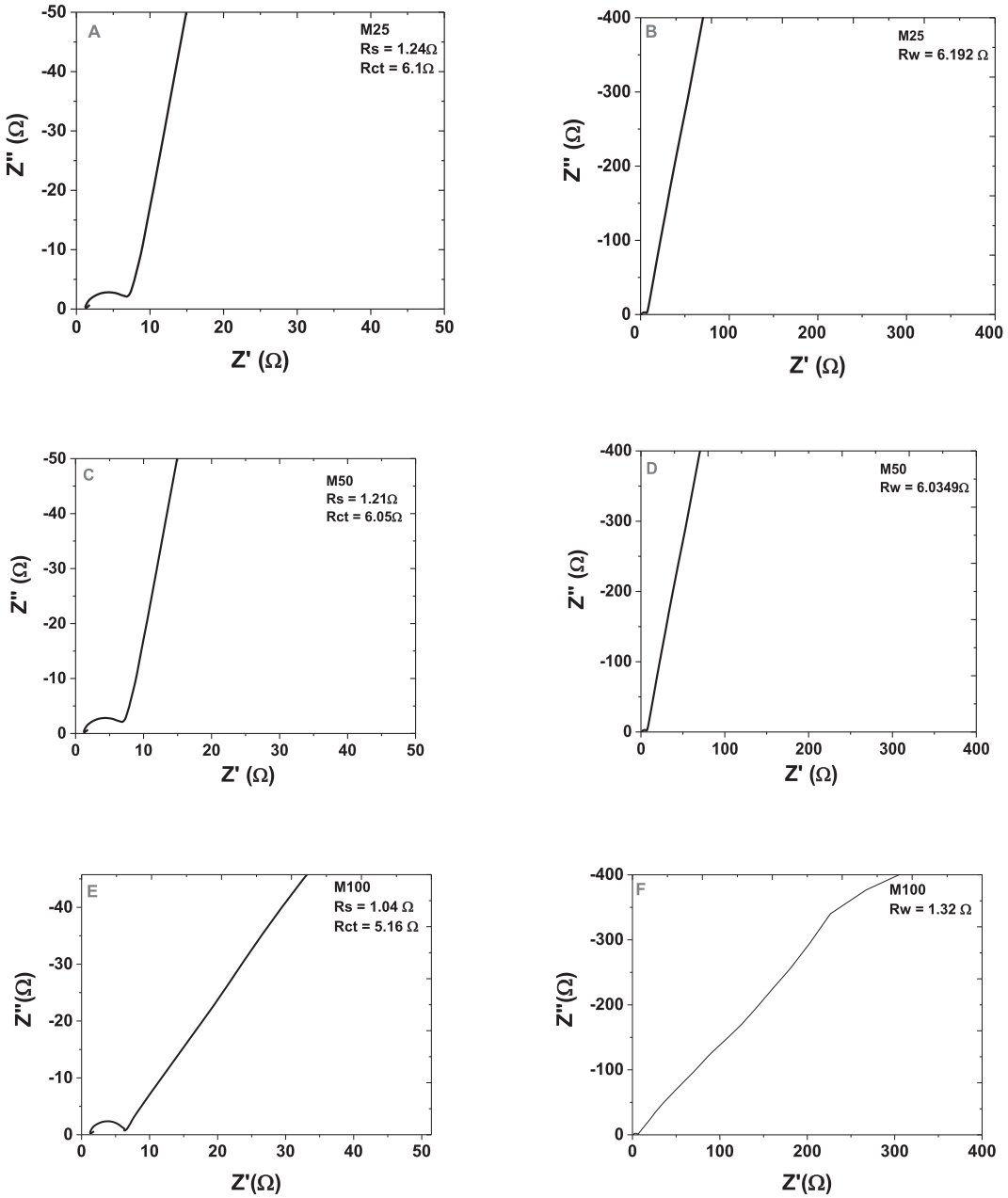

Fig. 6. A,C and E Nyquist plots of M_{25}, M_{50} and M_{100} in high frequency region. B,D and F Nyquist plots of M_{25}, M_{50} and M_{100} in low frequency region.

carried out (Figure 3A, B and C). It was found that the sample M_{100} exhibits lowest contact angle of 10° for water as liquid confirming the super-hydrophilic nature of M100 which is extremely supporting for the aqueous electrolytes. Bare (uncoated) SS strip exhibits a contact angle ~ 45°. As the pristine PPy material grows, the FE becomes more hydrophilic in nature from M25 to M100. This further corroborates that the increase in Py monomer concentration boosts the rate of polymerization and hence the growth of PPy.

3.3. Electrochemical analysis

3.3.1. Cyclic voltammetry

Prepared FEs M_{25}, M_{50}, and M_{100} were subjected to the cyclic voltammetry at 100 mVs^{-1}. The CV curves (Fiugre 4A) were used to calculate the capacitance (C), specific capacitance (SC) using the relations 1 and 2.

$$C = \frac{\int_{v1}^{v2} I\, dv}{V \frac{dV}{dt}} \quad (1)$$

$$SC = \frac{C}{m} = \frac{\int_{v1}^{v2} I\, dv}{m(V)\frac{dV}{dt}} \quad (2)$$

where, I is the average current in the Redox cycle, $V = V_2 – V_1$ is the potential window, dv/dt is potential scan rate, C is the capacitance, m is the weight of the active material immersed in the electrolyte. It was observed that the SC increases with the molar concentration of Py consumed during the synthesis. The variation is denoted at the inset of Fig. 4A. This could be due to the fact that with increase in molar concentration of consumed Py, the rate of polymerization increases. This increases the uni-dimensional growth of PPy matrix and amount of PPy matrix grown on the substrate forming more hydrophilic surface. Hence the SC might have enhanced with the increased molar concentration of Py. The charge storage occurs by doping and dedoping of anions in the PPy matrix hence as the matrix increases, the amount of charge stored increases and ultimately SC increases with increase in molar concentration of Py monomer consumed.

As M_{100} has produced maximum SC of 552.25 Fg^{-1}, the cyclic voltammetric analyses of C_2 at different potential scan rates from 5 mVs^{-1} to 100 mVs^{-1} has been carried out to study the effect of scan rate (Fig. 4B). Doping and dedoping of anions in the PPy matrix requires some time. The rate of change of potential is more than the speed of doping and dedoping of anions. Hence at high scan rate as the PPy matrix is unable to cope up with the rapid transitions in the potential applied, the fall in SC value was observed with increase in potential scan rate. The observed maximum SC was found to be 899.14 Fg^{-1} at 5 mVs^{-1}.

The cycling stability study of M_{100} has been carried at 100mVs^{-1} (Fig. 4C). It was observed that the value of SC initially falls down to 78% within first 100 cycles. Then it shows a constant decrease of 6% till the 500^{th} cycle where 62% of the retention of capacitance has been found. Then the SC remains almost unaltered. Even after 2000 cycles C_2 exhibits high stability with 61.5% retention in the SC.

3.3.2. Galvanostatic charge-discharge

Galvanostatic charge-discharge (GCD) analyses of FEs M_{25}, M_{50}, and M_{100} were carried out at 1 mA cm^{-2} constant current density (Fig. 5A). It was found that the SC goes on increasing with increase in the molar concentration of pyrrole monomer from M25 to M100. Here also as FE M_{100} gives maximum value of SC 738.41 F/g at 1 mA.

M_{100} was subjected to the different currents from 1 mA to 5 mA to study the effect of current density variations on the galvanostatic charge discharge behavior. From the charge discharge curves, SC values have been calculated using the relations 3.

$$SC = \frac{Id \times td}{mV} \quad (3)$$

where, V is the voltage, I_d and t_d are the discharging current and time, tc is the charging time, m is the mass of active material. The calculated values of SC at different currents are given at the inset of figure (Fig. 5B).

3.3.3. Electrochemical impedance spectroscopy

The EIS analyses of FEs M25, M50 and M100 have been carried out within the frequency range 1mHz–1MHz. The Nyquist plots at high frequency and low frequency are shown in figure 6A,C and E and 6B,D and F respectively. M100 has produced minimum values electrochemical series resistance (Rs), charge transfer resistance (Rct) and Warburg impedance (Rw) as those were 1.04Ω, 5.16Ω and 1.32Ω respectively. Densely grown FE M100 has properly interconnected globules which reduce the inter-particle resistance. Yet the small value of Rs is due to the resistance between the current collector and the grown material. Low Rct confirms that the grown material is highly adherent to the substrate. Low value of Rw is due to super-hydrophilic nature of M100 [15].

4. Conclusion

The molar concentration of pyrrole consumed during the synthesis of highly pristine PPy flexible electrodes affects growth hence the charge storage ability of the prepared FEs. With increase in molar concentration of monomer, the rate of polymerization increases and hence there is more growth of the material with increase in molar concentration. The increased amount of PPy results in more hydrophilic nature hence increased specific capacitance. The FE prepared with 0.1 M pyrrole exhibit specific capacitance as high as 899.14 Fg^{-1} in 0.2 M Na_2SO_4 electrolyte. Good electrochemical stability showing retention of 61.5% specific capacitance even after 2000 cycles has been observed.

Declarations

Author contribution statement

A. V. Thakur: Performed the experiments; Analyzed and interpreted the data.

B. J. Lokhande: Conceived and designed the experiments; Analyzed and interpreted the data; Contributed reagents, materials, analysis tools or data; Wrote the paper.

Funding statement

This research did not receive any specific grant from funding agencies in the public, commercial, or not-for-profit sectors.

Competing interest statement

The authors declare no conflict of interest.

Additional information

No additional information is available for this paper.

References

[1] G.A. Snook, A.S. Best, Review Conducting polymer based supercapacitor devices and electrodes, J. Power Sources 196 (2011) 1–12.
[2] L. Wang, C. Zhang, X. Jiao, Polypyrole based hybrid nanostructures grown on textile for wearable supercapacitors, Nano Res. 12 (5) (may 2019) 1129–1137.
[3] Yang Huang, Chunyi Zhi, Nanostrucutred Polypyrrole as a flexible electrode material of supercapacitor, Nano Energy 22 (2016) 422–438.
[4] H. Wang, Ze Xiang Shen, Polyaniline (PANi) bsed electrode materials for energy storage and conversion, J. Sci.:Adv. Mater. Dev. 1 (3) (2016) 225–255.

[5] M. Azimi, M. Abbaspour, A. Fali, B. Pourabbas, Investigation on electrochemical properties of Polythiophene nanocomposites with graphite derivatives as supercapacitor materials on breath figure decorated PMMA electrode, J. Electron. Mater. 47 (3) (2018) 2093–2102.
[6] A.V. Thakur, B.J. Lokhande, Morphological modification for optimum electrochemical performance of highly pristine polypyrrole flexible electrodes via SILAR immersion time and fabrication of solid state device, Port. Electrochim. Acta 36 (6) (2018) 37–392.
[7] S.S. Shinde, G.S. Gund, V.S. Kumbhar, B.H. Patil, C.D. Lokhande, Novel chemical synthesis of polypyrrole thin film electrodes for supercapacitor application, Eur. Polym. J. 49 (2013) 3734–3739.
[8] A.S. Liu, M.A.S. Oliveira, Electrodeposition of polypyrrole films on aluminum from tartrate aqueous solution, J. Braz. Chem. Soc. 18 (1) (2007) 143–152.
[9] P. Lemon, J. Haigh, The evolution of nodular polypyrrole morphology during Aqueous electrolytic deposition: influence of electrolyte Gas discharge, Mater. Res. Bull. 34 (5) (1999) 665–672.
[10] A.V. Thakur, B.J. Lokhande, Dip time dependent SILAR synthesis and electrochemical study of highly flexible PPy:$Cu(OH)_2$ hybrid electrodes for supercapacitors, J. Solid State Electrochem. 21 (9) (2016) 2577–2584.
[11] S. Visalakshi, R. Kannan, S. Valanarasu, H.S. Kim, A. Kathalingam, R. Chandramohan, Effect of bath concentration on the growth and photovoltaic response of SILAR-deposited CuO thin films, Appl. Phys. Mater. Sci. Process 120 (2015) 1105–1111.
[12] M.R. Das, A. Roy, S. Mpelane, Influence of dipping cycle on SILAR synthesized NiO thin film for improved electrochemical performance, Electrochim. Acta 273 (2018).
[13] M.M. Momeni, A.A. Mozafari, The effect of number of SILAR cycles on morphological, optical and photo catalytic properties of cadmium sulfide–titania films, J. Mater. Sci. Mater. Electron. 27 (2016) 10658.
[14] A.V. Thakur, B.J. Lokhande, Effect of precursor bath temperature on the morphology and electrochemical performance of SILAR-synthesized PPy:FeOOH hybrid flexible electrodes, Chem. Pap. 73 (4) (2019) 833–841.
[15] S. Choudhari, D. Bhattacharya, Jong-Sung Yu, 1-Dimensional porous α Fe_2O_3 nanorods as high performance electrode material for supercapacitor, RSC Adv. 3 (2013), 25120-251xx.